ResearchGate

See discussions, stats, and author profiles for this publication at: https://www.researchgate.net/publication/269275190

Generation and characterization of a novel human IgG1 antibody against vascular endothelial growth factor receptor 2

Article *in* Cancer Immunology and Immunotherapy · June 2014

DOI: 10.1007/s00262-014-1560-9

CITATIONS
15

READS
99

9 authors, including:

Juan Zhang
China Pharmaceutical University
62 PUBLICATIONS **461** CITATIONS
SEE PROFILE

Desmond Omane Acheampong
University of Cape Coast
59 PUBLICATIONS **155** CITATIONS
SEE PROFILE

Yuan He
University of Groningen
27 PUBLICATIONS **115** CITATIONS
SEE PROFILE

Min Wang
China Pharmaceutical University
150 PUBLICATIONS **1,600** CITATIONS
SEE PROFILE

Some of the authors of this publication are also working on these related projects:

humanized antibody View project

Monoclonal Antibody View project

All content following this page was uploaded by Juan Zhang on 14 June 2016.

The user has requested enhancement of the downloaded file.

Cancer Immunol Immunother (2014) 63:877–888
DOI 10.1007/s00262-014-1560-9

ORIGINAL ARTICLE

Generation and characterization of a novel human IgG1 antibody against vascular endothelial growth factor receptor 2

Wei Xie · Daojuan Li · Juan Zhang · Zhike Li · Desmond Omane Acheampong · Yuan He · Youfu Wang · Zhiguo Chen · Min Wang

Received: 6 December 2013 / Accepted: 16 May 2014 / Published online: 4 June 2014
© Springer-Verlag Berlin Heidelberg 2014

Abstract VEGF and its receptors, especially VEGFR2 (KDR), are known to play a critical role in angiogenesis under both physiological and pathological conditions, including cancer and angiogenic retinopathies. This study was aimed at developing a fully human IgG1 antibody (mAb-04) constructed from a phage-derived scFv, targeting the VEGF/VEGFR2 pathway. Firstly, an innovative transfection system, containing two recombinant expression vectors (pMH3 and pCApuro), were introduced into CHO-s cells and clones with higher yield selected accordingly. After an optimal fermentation condition was determined, fed-batch fermentation was performed in 5-L bioreactor with a final yield up to 60 mg/L. Further, cell proliferation, wound healing, transwell invasion, tube formation and chick embryo chorioallantoic membrane assays showed significant anti-angiogenic activity of mAb-04 in vitro and in vivo. In addition, the results of Western blotting indicated the ability of mAb-04 to inhibit VEGF-induced VEGFR2 signaling pathway. Finally, ADCC assay demonstrated that mAb-04 is capable of mediating tumor cell killing in presence of effector cells. This study has therefore proved that the full-length antibody targeting human VEGFR2 has potential clinical applications in the treatment of cancer and other diseases where pathological angiogenesis is involved.

Keywords VEGFR2 (KDR) · Human monoclonal antibody · CHO cell line · Anti-angiogenesis · ADCC

Abbreviations

ADCC	Antibody-dependent cellular cytotoxicity
bFGF	Basic fibroblast growth factor
CAM	Chick embryo chorioallantoic membrane
ECGS	Endothelial cell growth supplement
ECM	Endothelial culture medium
FBS	Fetal bovine serum
HAMA	Human anti-mouse antibody
KDR	Kinase insert domain-containing receptor
KDR3	The extracellular domain 3 of human VEGFR2
LDH	Lactate dehydragenase
scFv	Single-chain antibody fragment
VEGF	Vascular endothelial growth factor
VEGFR2	Vascular endothelial growth factor receptor 2

Introduction

Monoclonal antibodies were initially produced using the hybridoma technique in which a murine plasma cell is immortalized by fusing it with a plasmacytoma-derived cell line that will grow continuously in culture [1–3]. But the mouse hybridoma-derived antibodies can be recognized by human immune system as foreign resulting in HAMA response, leading to shortened half-life, reduced efficacy and increased toxicity in some patients [4, 5]. To reduce the immunogenicity of the murine antibodies, recombinant

The authors Wei Xie and Daojuan Li contributed equally to this work.

Electronic supplementary material The online version of this article (doi:10.1007/s00262-014-1560-9) contains supplementary material, which is available to authorized users.

W. Xie · D. Li · J. Zhang (✉) · Z. Li · D. O. Acheampong · Y. He · Y. Wang · Z. Chen · M. Wang (✉)
State Key Laboratory of Natural Medicines, School of Life Science and Technology, China Pharmaceutical University, 154#, Tong Jia Xiang 24, Nanjing 210009, People's Republic of China
e-mail: juancpu@126.com

M. Wang
e-mail: minwang@cpu.edu.cn

DNA technologies were used to make chimeric antibodies. However, the resulting antibodies still contained potentially immunogenic murine sequences [6, 7]. More recently, fully human antibodies have been generated using transgenic mice expressing human Ig repertoire or be derived from phage displayed scFv or Fab antibody formats [8–10]. However, the "humanized" mice producing fully human antibodies upon immunization are not available to all investigators. In contrast, phage display is readily available at lower cost [11].

Due to their common deficiency of short half-life caused by small molecular size (less than 30 KD), none of the invented phage displayed scFvs has been put into clinical use before further engineering processing. It would be necessary to integrate the robust avidity, effector functions and the prolonged serum half-life by transferring the antigen-binding property of the scFv into a full-length IgG antibody.

The VEGF–VEGFR interaction functions as an up-regulator in tumor angiogenesis and metastasis. Evidence suggests that VEGFR2 can mediate endothelial cell proliferation and is an important mediator in angiogenesis [12–14]. Inhibition of angiogenesis with antagonists to either VEGF or KDR has led to significant therapeutic efficiency both in preclinical animal models and in clinical trials [15]. Since 2004, Bevacizumab has been the only antibody drug on the market targeting VEGF-KDR signal pathway. However, available clinical data show that blocking of VEGF by Bevacizumab does not completely inhibit tumor angiogenesis. Therefore, the development of additional antibodies targeting VEGFR2 is required for more effective treatment of tumors through VEGF-KDR pathway.

We previously generated a scFv antibody (AK404R) targeting KDR3 from a phage display library [16]. Considering the short half-life of scFv, here we generated fully human IgG1 antibody (mAb-04) from AK404R. Monitoring its real-time binding to KDR3 by Biacore was first executed to detect the affinity of mAb-04 in vitro. The ability of mAb-04 to inhibit angiogenesis was shown by its effect on proliferation, migration, invasion and tube formation of HUVECs. It competed efficiently with VEGF for binding to KDR and blocked VEGF-stimulated mitogenesis of HUVECs [12, 17–20]. Additionally, the direct antitumor activity of mAb-04 was demonstrated using the ADCC assay. Thus, mAb-04 is expected to provide as a novel antiangiogenic therapeutic antibody.

Materials and methods

Cell culture

The Chinese hamster ovary cell line CHO-s (Amprotein Co., Ltd, Hangzhou, China) was maintained in DMEM/F12 medium, supplemented with 10 % (v/v) FBS. The serum-free medium B001 and F001 for suspension culture and fermentation of CHO-s cells were purchased from Amprotein Co., Ltd. Mouse macrophage cell line RAW264.7, mouse embryonic fibroblast cell line 3T3-L1 and human embryonic kidney cell line HEK293 preserved in our lab were cultured in DMEM medium (high glucose), supplemented with 10 % (v/v) FBS. The mouse melanoma cell line B16F10 preserved in our lab was cultured in RPMI 1,640 medium containing 10 % (v/v) FBS. Cell culture media, supplements and trypsin powder were purchased from Life technologies (Basel, Switzerland). HUVECs purchased from ScienCell Research Laboratories were cultured in ECM supplemented with 5 % (v/v) FBS and 1 % (v/v) ECGS (ScienCell, San Diego, CA).

Construction of the expression plasmids and selection of stable transfected cells

PCR mastermix was purchased from Biotek (Beijing, China). Restriction and modification enzymes were from Takara (Otsu, Japan) or NEB (New England Biolabs, USA). Eukaryotic expression vectors pMH3 and pCApuro were purchased from Amprotein Co, Ltd. The heavy and light chain genes were prepared separately according to the amino acid sequence of scFv-AK404R we reported. Firstly, the DNA sequences were optimized to remove the cleavage sites. Suitable light chain constant region (CL) and heavy chain constant region1 (CH1) were obtained from the GenBank and synthesized. After an optimization to CHO-preferred codons in heavy and light chain variable regions (VH and VL), CL was linked to 3′ end of VL (5′-actgctgctctgggttccaggttccactggtctgcaatccgtgctgaccc-3′ and 5′-gagagagacacactcctgctatgggtactgctgctctgggttccag-3′), while CH1 to 3′ end of VH (5′-tatacccaagcttgccaccatg-3′and 5′-atagtttagcggccgcaaccttct-3′) by overlap PCR. Then, CH1-VH was linked to Fc fragment by T4 DNA ligase. The human IgG1 Fc fragment is preserved in our lab. Finally, the Kozak sequence (AAGCTTGCCACC), cleavage sites and signal peptide were added to the N-terminal of VH (5′-cccccaagctggaattccaccatggagagagacacactcctgc-3′ and 5′-ttttccttttgcggccgcttattacctggagacagggagagg-3′) and VL (5′-cccccaagctggaattccaccatggagagagacacactcctgc-3′ and 5′-ttttccttttgcggccgcttagctgcactcagcaggggcg-3′). After digestion with *Not*I and *Eco*RI, the amplified DNA and pMH3/pCApuro fragments were joined. Nucleotide sequence of the recombinant vectors (H-chain and L-chain) was confirmed by Meiji Co, Ltd. (Shanghai, China).

The four recombinant expression vectors (pMH3-H, pMH3-L, pCApuro-H and pCApuro-L) were transfected into CHO-s cell line with the same number of moles by electroporation. The stable transfectants were then screened with 1 mg/mL G418 (Sigma-Aldrich, St. Louis, USA), and the high-yield clones selected by Dot blot (HRP conjugated

goat anti-human IgG Fc, Sino Biological Inc., China) and Western blot assay (HRP conjugated goat anti-human IgG H+L, Sino Biological Inc., China).

Expression and purification of mAb-04

Three prior clones with higher production were inoculated separately into sealed 40-mL-bioreactor-like flasks at 37 °C with a rotation speed of 120 rpm. Exponentially growing cells harvested from 40 mL shake flasks were inoculated at 2.5×10^6 cells/mL into a 3 L bioreactor. Protein expression was induced at 34 °C when cell density reached 5–8 $\times$ 10^6 cells/mL. The fermentation was monitored by daily changing 3 % medium and supplementing proper amount of glucose. The supernatant samples were collected when cell viability was beneath 70 % and then purified using Protein A affinity chromatography (GE Healthcare, Buckinghamshire, UK). The integrity of the full-length mAb produced by different clones was determined by ELISA. Finally, one prior clone chosen for mass mAb-04 production was harvested from 40-mL shake flasks and inoculated in a 5-L wave bioreactor for fermentation.

Binding affinity and kinetic analysis

The binding kinetics of mAb-04 to KDR was measured with Biacore system (Biacore X100, GE Healthcare, Sweden). Firstly, anti-human IgG (Fc) antibody was immobilized on Sensor Chip CM5 using Human Antibody Capture Kit (GE Healthcare, Sweden). Next, mAb-04 was captured by the anti-human IgG (Fc) antibody, and the target resonance unit (RU) density was 2000. Finally, soluble recombinant KDR3 protein was injected at different concentrations into running buffer (HBS-EP, pH 7.4), and capture was done at a constant flow rate of 30 μL/min at 25 °C. Meanwhile, one flow cell of the sensor chip was left without captured mAb-04 to provide a reference surface. Captured antibodies together with any analyte bound to them were removed by flowing regeneration solution (3 M magnesium chloride) at 30 μL/min for 30 s. Sensorgrams were obtained at each concentration and evaluated with Bivalent analyte, to determine the association rate constant k_a and dissociation rate constant k_d. The equilibrium dissociation constant (K_D) was calculated from the ratio of rate constants k_d/k_a.

Flow cytometry assay

4×10^5 KDR over-expressing HUVECs or KDR-negative HEK293 cells per sample were suspended in PBS containing 5 % BSA and then incubated with/without 200 μg/mL mAb-04 or the control VEGFR2 rabbit mAb (Cell Signaling, USA) at 4 °C for 1 h. Cells were then incubated with FITC-conjugated goat anti-human IgG antibody or FITC-conjugated goat anti-rabbit antibody (SANGON, Shanghai, China). Finally, the cells were washed and the binding assay was performed with a BD FACS flow cytometer.

Cell proliferation assay

4×10^3 HUVECs and HEK293 cells were seeded into a 96-well plate to attach for 24 h, then different concentrations of mAb-04 were added and pre-incubated at 37 °C for 1 h, after which $VEGF_{165}$/bFGF was added at a final concentration of 10 ng/mL. The mAb-04 untreated group with VEGF/bFGF induced was as a vehicle control. Sunitinib (adamas-beta, Shanghai, China) was used as positive control. After incubation for 24, 48 and 72 h, cell viability was quantified by MTT assay and the inhibitory rates were expressed as percentages of the vehicle control (100 %). The IC_{50} values were then calculated by curve fitting.

Wound healing assay (scratch assay)

2×10^5 HUVECs were placed into 12-well plate and then starved by serum-free ECM for 12 h. The monolayer cells were scratched with a 1-mL pipette tip. Whereafter, different concentrations of mAb-04 (0, 10, 50 and 200 nM) were added. Following 0, 12, 16, 20, 24 h incubation, images were taken with OLYMPUS fluorescence microscope. The wound migrated distances were measured with Image-Pro-Plus program and calculated as follows: $Ln = \frac{L0-Ltime}{2}$.

Transwell invasion assay

1×10^4 HUVECs and various concentrations of mAb-04 (0, 10, 50 and 200 nM) suspended in serum-free medium was added to the top 24-well transwell chambers (Millipore, Billerica, USA) coated with 20 μL Matrigel. The bottom chambers were filled with 600 μL ECM containing 5 % (v/v) FBS and 1 % (v/v) ECGS. After 12-h incubation, non-invasive cells on the top surface of the membrane were removed with cotton swabs. The invaded cells were then fixed with 4 % polyoxymethylene for 20 min and washed thrice by PBS. The cells were stained with 1 % (w/v) crystalline violet and washed thrice with distilled water. Images were taken using an OLYMPUS inverted microscope at 100-times magnification. Invaded cells were counted using Image-Pro-Plus program and invasion percentages quantified on the basis of mAb-04 untreated control.

Tube formation assay

Matrigel (BD Biosciences) was thawed on ice for 24 h, then 50 μL aliqouts per well was coated into a 96-well tissue culture plate and incubated at 37 °C for 1 h to

solidify. 2×10^4 HUVECs were seeded into the 96-well plate and added with 100 μL ECM supplemented with 2 % (v/v) FBS, 1 % (v/v) ECGS and different concentrations of mAb-04 (0, 10, 50 and 200 nM). After 8-h incubation, endothelial tube formation was photographed with an inverted OLYMPUS microscope at 100-times magnification. The endothelial tubes were counted with Image-Pro-Plus program.

CAM assay

Group of 20 fertilized 8-day-old chick embryos (Nanjing Medical Device Factory) were incubated at 37 °C with 70 % humidity. A window (about 1.5 cm × 1.5 cm) was created on the egg shell to expose the chorioallantoic membrane. Gelatin sponges (about 5 mm × 5 mm) loaded with different concentrations of mAb-04 (0, 10, 50 and 200 nM) were placed on the CAMs. After being incubated and fixed, each piece of CAM was carefully taken out and transferred to a cover slip and photographed with a Canon camera. The blood vessel branch points were counted with Photoshop program to quantify the neovascularization activity.

Western blot assay

2×10^5 HUVECs were seeded into a 6-well plate, treated with series of concentrations of mAb-04 (0, 10, 50 and 200 nM) for 1 h after starvation and then stimulated with 10 ng/mL VEGF for another hour. The whole cell extracts were harvested using RAPI buffer (Beyotime, Shanghai, China). Proteins were resolved by electrophoresis then transferred onto PVDF membranes. The membranes were blocked and incubated with primary antibodies anti-β-actin (Anbo, USA), anti-VEGFR2 (EPITOMICS, CA), anti-VEGFR1 (Cell Signaling, USA), anti-AKT (Cell Signaling, USA), anti-P38 MAPK (Anbo, USA), anti-ERK1/2 (EPITOMICS, CA), and phosphor-specific anti-VEGFR2 (Tyr^{1175}) (Cell Signaling, USA), anti-VEGFR1 (Tyr^{1213}) (Anbo, USA), anti-AKT (Ser^{473}) (EPITOMICS, CA), anti-P38 MAPK (Thr^{180}/Tyr^{182}) (Cell Signaling, USA) and anti-ERK1/2 (Tyr^{202}/Tyr^{187}) (EPITOMICS, CA) at 4 °C overnight. After being washed, the membranes were incubated with corresponding secondary anti-mouse/anti-rabbit antibodies conjugated to horseradish peroxidase (HRP). The membranes were reacted with enhanced ECL chemiluminescence reagent (Millipore, Billerica, USA) and exposed by Bio-Rad detection system.

ADCC assay

The CytoTox 96 nonradioactive cytotoxicity assay (Promega, Madison, USA) was performed based on the calorimetric detection of LDH released from the target cells B16F10 (KDR high-level expression cell line) or 3T3-L1 (controlled cell line). A murine macrophage-like cell line RAW264.7 served as effector cells. Either 5×10^3 B16F10 cells or 3T3-L1 cells were co-cultured with various amounts of RAW264.7 cells in the presence or absence of mAb-04/AK404R for 5 h at 37 °C. Subsequently, 50 μL of supernatants was assayed for LDH activity following manufacturer's protocol. Controls for spontaneous LDH release in effector and target cells, as well as target maximum release, were prepared. The calculation of cytotoxicity percentage was as follows:

$$\%\ \text{cytotoxicity} = \frac{(\text{experimental} - \text{effector spontaneous} - \text{target spontaneous})}{(\text{target maximum} - \text{target spontaneous})} \times 100.$$

Statistical analysis

The data were analyzed using Excel and SPSS 17.0 software. Results are presented as the mean ± SD from at least three independent experiments. The *t* test was used to compare the inhibitory rates of different samples in MTT assay, transwell invasion assay et al. A p value <0.05 was considered statistically significant. All figures were produced with GraphPad Prism 5 software program.

NCBI accession numbers of CL, CH1 and human IgG1 Fc are NM_152855.1, AAX09633.1 and AF150959.1, respectively.

Results

Construction of the expression plasmids and selection of stably transfected clones

We generated a full-length antibody from the DNA sequence of anti-VEGFR2 scFv and the human IgG1 Fc fragment, with the predicted molecular weight of 150 KD. The pCApuro (ampicillin resistance) and pMH3 (ampicillin and neomycin resistance) vectors were employed as the expression vectors (Fig. 1a).

CHO-s cells at exponential growth were successfully transfected by electroporation method and screened with G418 (1 mg/mL) containing medium. Four clones with higher expression level were chosen from 200 clones randomly picked from dishes and subcultured in dishes for the second round of screening (Supplementary Fig. 1). Finally, stably transfected cell lines with higher yield (B3, C2, C4 showed in Fig. 1b) were obtained. Further characterization of the secreted products of the three clones by Western blot showed that they were making H and L chains of the expected molecular weight (Fig. 1d) that were mostly assembled into complete antibodies of 150 KD with some

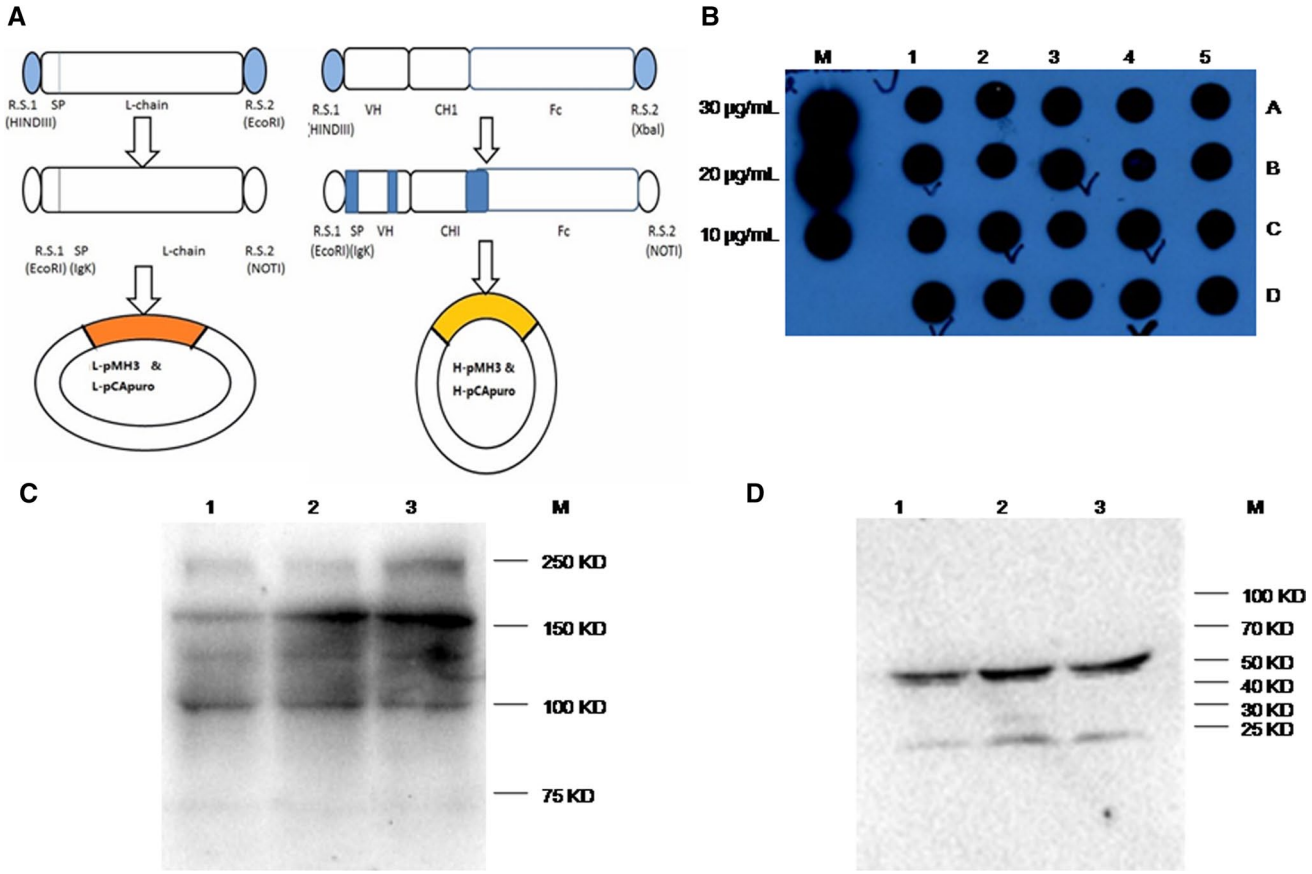

Fig. 1 **a** Flow diagram for the construction of expression plasmids. Signal peptide (SP, Ig kappa, NCBI accession number: AAA38778.1) and restriction enzyme (*Eco*RI and *Not*I) recognition sites were appended both in H-chain and in L-chain. **b** Semi-quantitative determination of the target protein. Anti-IL 12 human IgG1 antibody was set as the standard substance. Three preferable clones (B3, C2, and C4 of about 10 μg/mL) in the 24-well plate were confirmed and named Clone 1, Clone 2, and Clone 3, respectively. **c, d** Western blot analysis (under non-reducing and reducing condition, respectively) for 24-h cultured high-yield clones.*M*: Marker; *lane 1*: Clone 1; *lane 2*: Clone 2; *lane 3*: Clone 3

incompletely assembled proteins of 125 and 100 KD (Fig. 1c). The three clones which produced approximately 10–20 mg/L of antibody were expanded into serum-free suspension culture for the production of mAb-04.

Expression and purification of mAb-04

To determine the suitable clone for large-scale fermentation, the viability and production of the three clones were examined in 3-L bioreactor. Samples were taken daily for cell viability assay and production determined with ELISA. Clone 1 with relatively lower expression level was discarded. Clone 2 achieved its peak cell density (8.1×10^6 cells/mL) at day 11, while Clone 3 achieved a relatively higher peak cell density (9.7×10^6 cells/mL) at day 10 (Fig. 2b). The production of Clone 3 reached a peak value of 62.8 mg/L, while the production of Clone 2 reached a peak value of 48.3 mg/L. Both Clone 2 and Clone 3 reached the production of 6.88×10^{-9} g per cell. Considering the fact that Clone 3 has the potential to achieve greater cell density, it was chosen for further scale-up fermentation. During the enlarged fermentation in a 5-L bioreactor, time course of viable cell density, cell viability and antibody production throughout the whole fermentation process was monitored (Fig. 2c). The density of inoculated viable cells at the beginning of fermentation was 2×10^6 cells/mL. After 12-day fermentation, the final yield reached 77 mg/L. The cell viability measured at days 4, 6, 7, 8 and 12 were 95.0, 91.6, 93.6, 90.2 and 86.1 %, respectively. Glucose consumption had a positive correlation with cell density and production of mAb-04. Thus, mAb-04 production by the CHO-s cells was non-growth-associated, and large amount of mAb-04 was secreted during the stationary phase.

SDS-PAGE analysis of purified product from 5-L fermentation showed product containing two monomers (H-chain and L-chain) under reducing condition (Fig. 2d, lane 6, 7) and formed homodimers under non-reducing

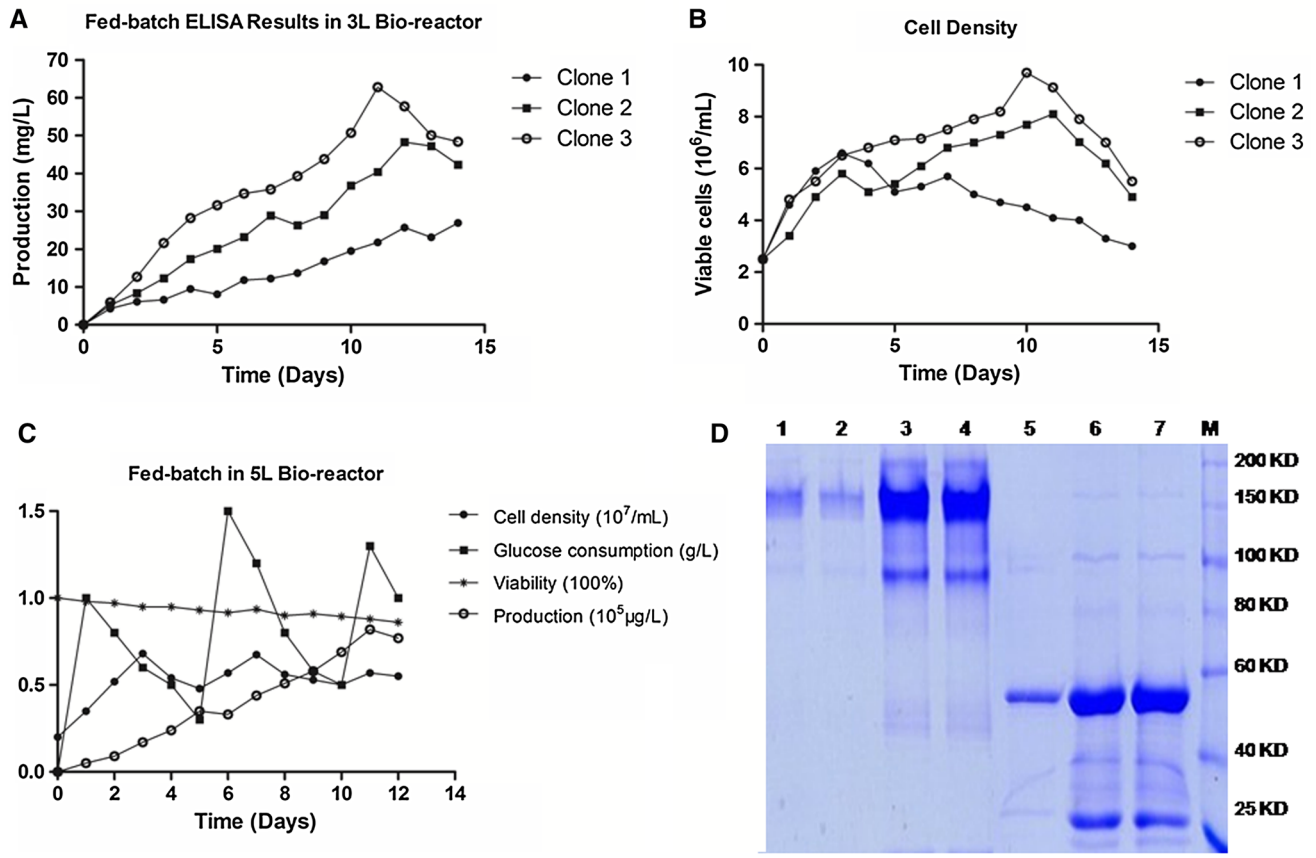

Fig. 2 **a, b** The determination of mAb-04 production and profile of cell viability assay for three prior clones in 3-L bioreactor. **c** Fed-batch fermentation of Clone 3 in 5-L bioreactor. **d** SDS-PAGE analysis for purified product of the fermentation. *Lane M*: Marker; *lane 1*: Elution peak (pH 3.5); *lanes 2 and 5* Elution peak (digested to pH 7.1, *lane 2* represented non-reducing and *lane 5* represented reducing condition); *lanes 3 and 6* Condensed samples in non-reducing and reducing condition; *lanes 4 and 7*: Condensed samples after filtration in non-reducing and reducing condition

condition (Fig. 2d, lane 3, 4). These results suggested that the mAb-04 was expressed and folded as a homodimer, which was the main component of the purified product. The final yield after filtration presented a small loss which can be detected from the difference between lane 3 and lane 4, or lane 6 and lane 7. These results indicated we have obtained a full-length antibody product with more than 90 % purity (SDS-PAGE grade) as per Imager photograph quantification.

Affinity and binding kinetics

We chose to use the 2:1 binding model after preliminary evaluation of the fit of binding curve using several models incorporating varying ratios of interaction revealed that the 2:1 binding model exhibited the best *U*-value for interaction of mAb-04 and KDR3 (Fig. 3b, c).

As anticipated, KDR3 showed concentration-dependent affinity to mAb-04 (Fig. 3a). The ka was $1.82 \times 10^6\ M^{-1}\ s^{-1}$; this value indicated a fast association between mAb-04 and KDR3. The dissociation rate constant also pointed to a relatively stable process for KDR3 dissociation from the immobilized mAb-04 with the value $2.68 \times 10^{-3}\ s^{-1}$. The equilibrium dissociation constant (KD) calculated from the ratio of rate constants kd/ka was 1.47×10^{-9} M. In general, KDR3 exhibited specificity and high affinity to immobilized mAb-04 under the given experimental conditions, which accordingly attested to the strong binding ability with antigen of mAb-04 in vitro.

Flow cytometry analysis

Compared with the KDR-negative cell line HEK293, mAb-04 demonstrated relatively high binding signals with HUVECs (Fig. 3d, e). The binding rates of 200 μg/mL mAb-04 with HUVECs and HEK293 cells were 46.0 and 2.13 %, respectively. Also the binding rate of control VEGFR2 rabbit mAb with HUVECs and HEK293 cells was 76.8 and 2.61 % respectively. The results indicated that mAb-04 combined with HUVECs with a relatively high binding rate.

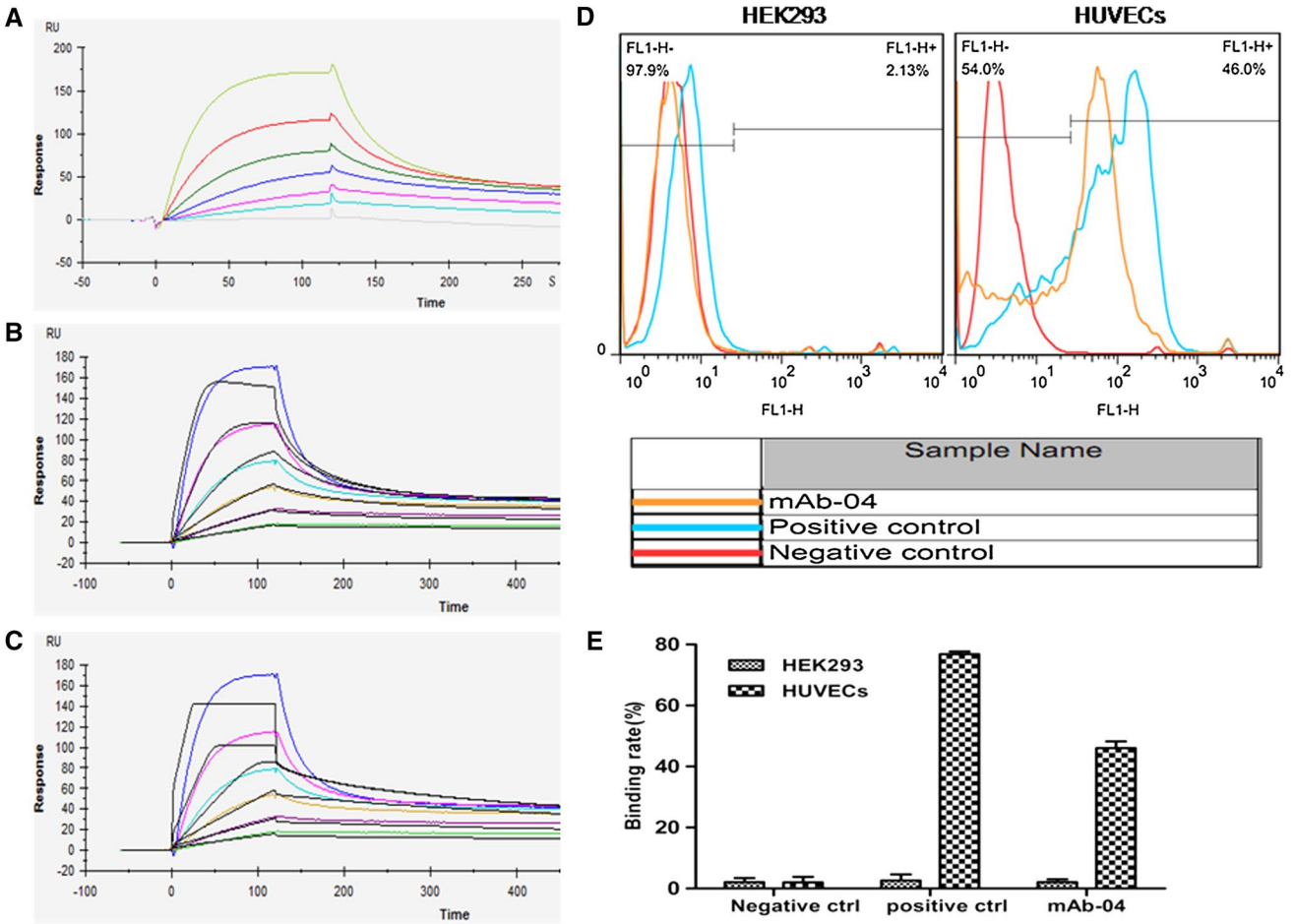

Fig. 3 **a** Set of sensorgrams of KDR3 binding with mAb-04. Experimental results for the real-time binding of KDR3 to immobilized mAb-04 showed that the association rate increased with increasing concentration of the KDR3 (from *bottom* to *top*), ranging from 2.5 to 80 nM. The *bottom line* of sensorgrams served as a reference surface. The complex dissociated when buffer flowed through at 120 s. **b, c** *Fitted curve* of KDR3 binding with mAb-04. **b** *Fitted curve* of 2:1 binding model. The *U*-value analyzed by BIAcore X100 Evaluation software was 14. **c** Fitted curve of 1:1 Langmuir binding model. The *U*-value analyzed by BIAcore X100 Evaluation software was 65. **d, e** mAb-04 demonstrated relatively high binding signals with HUVECs than KDR-negative HEK293 cells

mAb-04 inhibits HUVECs proliferation, migration and invasion

MTT and wound healing assays were performed to determine the effects of mAb-04 on HUVECs proliferation and migration [12, 20–23]. Results showed that the inhibition of mAb-04 on proliferation of HUVECs was time- and dose-dependent (Fig. 4a, b). After 24, 48 and 72 h effect of mAb-04 with 10 ng/mL VEGF induced, the IC_{50} values were ~92.72, ~62.75 and ~71.03 nM, respectively. The IC_{50} value of sunitinib on HUVECs was ~61.252 nM after 72 h incubation. The inhibition of mAb-04 on HUVECs with bFGF induced was not obvious (Fig. 4b). The results indicated that mAb-04 can effectively and specifically inhibit the proliferation of VEGF-stimulated HUVECs.

The influence of mAb-04 on HUVECs migration was investigated through scratch assay. As shown in Fig. 4c, d, the gap width of mAb-04 untreated control group narrowed more vividly than mAb-04 treated groups from 0 to 24 h, indicating that mAb-04 could time- and dose-dependently weaken the migration capability of endothelial cells, and we also found that 50 and 200 nM mAb-04 can strongly inhibit the migration of HUVECs.

As endothelial cells invasion is a critical aspect of angiogenesis, transwell invasion assays were performed to estimate the ability of inactivated HUVECs to pass through the transwell membrane barrier in the presence or absence of mAb-04. As shown in Fig. 4e, f, the invasive cells to the lower chamber were significantly reduced with increasing concentration of mAb-04. The inhibitory rate of 200 nM

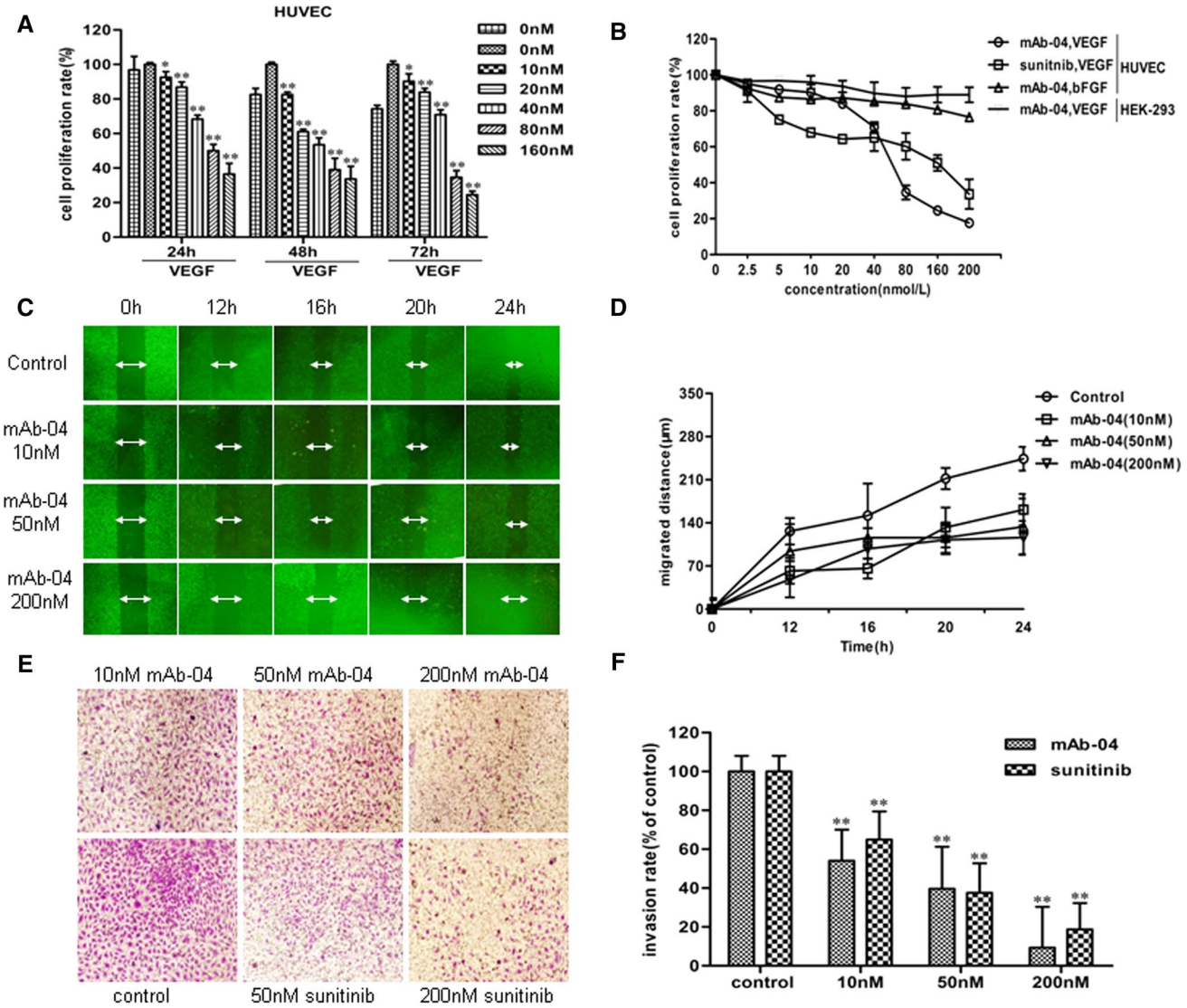

Fig. 4 **a, b** mAb-04 and sunitinib specifically inhibited the proliferation of HUVECs with VEGF stimulated in dose- and time-dependent manner. **c** Photomicrographs of wound healing assay showing that mAb-04 dose-dependently decreased the migration of HUVECs. **d** Quantitative analysis of the wound healing assay revealing that mAb-04-treated HUVECs migrated more slowly after wounding. **e** Photomicrographs of transwell invasion assay showing that mAb-04 could effectively inhibit the invasion of endothelial cells. **f** Quantitative analysis of the transwell invasion assay indicating that mAb-04 suppressed the invasion of HUVECs in dose-dependent manner (Data were presented as the mean ± SD, $n = 5$, $^{*}p < 0.05$, $^{**}p < 0.01$, vs. mAb-04 untreated group)

mAb-04 on invasion of HUVECs was 90.61 %, whereas the rate of 200 nM sunitinib was 81.28 %.

mAb-04 inhibits VEGF-induced capillary structure formation of HUVECs

Although angiogenesis is a complex procedure of several kinds of cells, the maturation of endothelial cells into a capillary tube is a critical early step [17–19, 24, 25]. Tube formation assay was performed to determine the effect of mAb-04 on HUVECs tube formation. As shown in Fig. 5a, b, capillaries were gradually abrogated due to increasing mAb-04 concentrations. Almost 90 % destruction of tube network was observed when HUVECs were incubated with mAb-04 at 200 nM.

mAb-04 suppresses the angiogenesis in vivo

The CAM model was performed to determine the potential anti-angiogenic activity of mAb-04 in vivo. As shown in Fig. 5c, d, new blood vessels were formed on CAMs in mAb-04 untreated control group. After incubation for 72 h, mAb-04 slightly inhibited chicken embryonic blood vessel formation around the gelatin sponge at the concentration

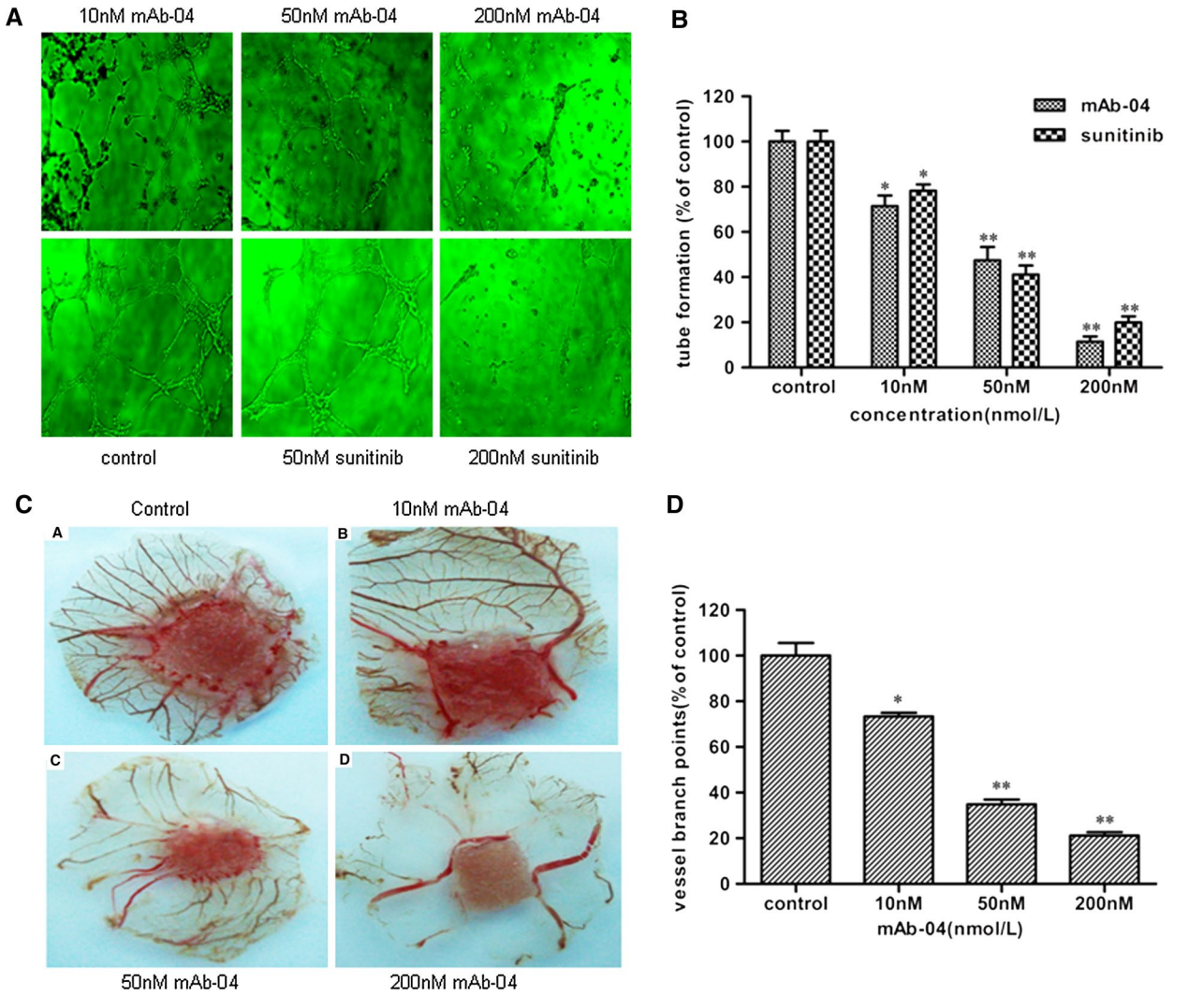

Fig. 5 **a** HUVEC tube-like photomicrographs showing the significant effects of mAb-04 on HUVECs tube formation. **b** Quantitative analysis demonstrating that 50 nM mAb-04 inhibited approximately 50 % tube formation of HUVECs on Matrigel, and 200 nM mAb-04 inhibited tube formation of HUVECs significantly with the inhibitory rate reaching 88.6 %. (Data were presented as the mean ± SD, $n = 5$, $^{*}p < 0.05$, $^{**}p < 0.01$, vs. untreated control). **c** Photographs of chicken chorioallantoic membrane assay showing that mAb-04 inhibited the microvessels formation of CAM model in a dose-dependent manner. **d** Statistical analysis of CAM assay revealing 50- and 200-nM mAb-04 inhibited chicken embryonic blood vessel formation around the gelatin sponge significantly after 72-h incubation, demonstrating that mAb-04 was able to suppress angiogenesis in embryos

of 10 nM, whereas 50 and 200 nM mAb-04 drastically inhibited neovascularization of the CAM, accompanied by a lack of prominent vessel networks. This result demonstrated that mAb-04 was able to suppress angiogenesis in embryos.

mAb-04 inhibits VEGF-induced VEGFR2 signaling pathway

Previous studies indicated that blockage of VEGFR2 activity could significantly limit tumoral neo-angiogenesis process [20, 23]. We first examined the effect of mAb-04 on tyrosine phosphorylation of VEGFR2 activated by VEGF. As shown in Fig. 6a, mAb-04 dose-dependently inhibited the phosphorylation of VEGFR2.

VEGFR2 regulates endothelial cells proliferation and migration by regulating the activation of ERK and P38 MAPK. To investigate the inhibitory effects of mAb-04 on HUVECs proliferation and migration, the effects of mAb-04 on the phosphorylation of ERK and P38 MAPK were examined. As shown in Fig. 6a, mAb-04 significantly interfered with the phosphorylation of both ERK and P38 MAPK, suggesting that mAb-04 inhibited cell proliferation and migration of endothelial cells by suppressing VEGFR2 and the activities of its downstream protein kinase. The phosphorylation of Tyr1175 of VEGFR2 mediates the

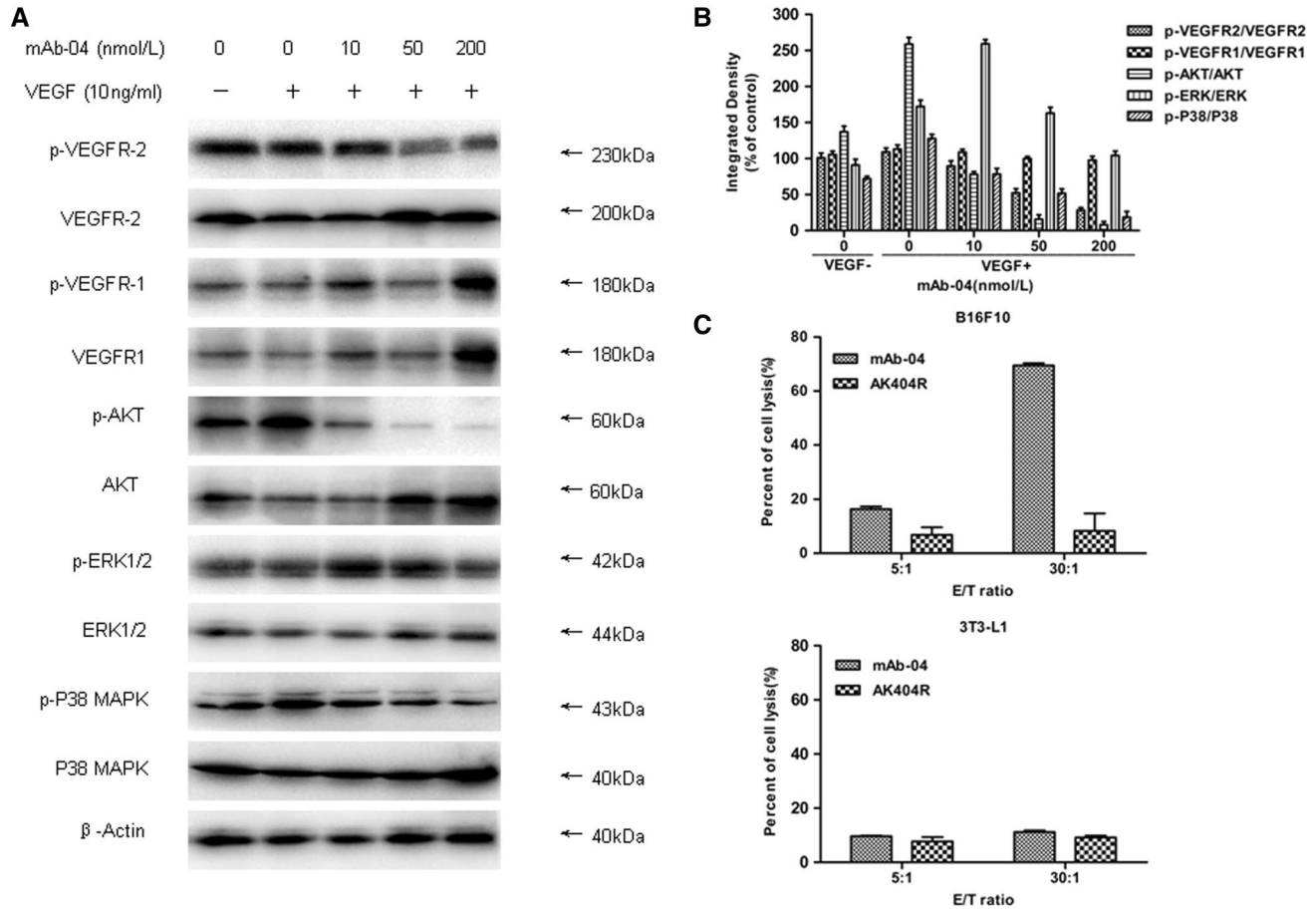

Fig. 6 **a** Western blotting results showing that mAb-04 dose-dependently and specifically inhibited VEGF-induced phosphorylation of VEGFR2 and suppressed VEGFR2-mediated downstream protein kinase activation of AKT, ERK and P38 MAPK. **b** Percentages of p-VEGFR2/VEGFR2, p-AKT/AKT, p-ERK/ERK and p-P38/P38 indicating that mAb-04 inhibited VEGFR2-mediated signaling cascade in dose-dependent manner. **c** The ADCC activity of mAb-04. Cytotoxity was determined by measuring the released LDH. The cytotoxity of B16F10 co-cultured with mAb-04 enhanced obviously when the E/T ratios increased

activation of AKT to regulate cell proliferation [20]. To further determine the downstream signaling pathways mediated by VEGFR2, the activation of AKT was examined. As shown in Fig. 6a, b, mAb-04 dose-dependently inhibited the phosphorylation of AKT signaling pathways. Statistical analysis shown in Fig. 6b corroborated the results. The inhibition tendency of different concentrations of mAb-04 on VEGFR2-mediated signaling cascade can be found from the percentages of p-VEGFR2/VEGFR2, p-AKT/AKT, p-ERK/ERK and p-P38/P38.

Cytotoxicity assay of mAb-04

To determine the ability of Fc fragment of mAb-04 to trigger significant effector cell-mediated lysis, ADCC study on KDR high-level expression cancer cells was employed. The single chain fragment AK404R that lacks Fc fragment did not significantly enhance the lysis of either KDR high-level expression B16F10 cells or 3T3-L1 cells (as controlled). Figure 6b showed mAb-04 relatively enhanced the lysis of KDR high-level expression B16F10 cells. Approximately 15 % of the KDR high-level expression B16F10 cells were lysed when presented in an E/T (effective cells/target cells) ratio of 5:1 with 30 μg/mL mAb-04. The antibody-specific lysis increased to 70 % at the higher E/T ratio of 30:1. However, mAb-04 did not enhance the lysis of the 3T3-L1 cells. These results demonstrated that mAb-04 specifically enhanced the ADCC of KDR high-level expression cancer cells.

Discussion

We have previously reported a novel human scFv against KDR3 [16, 26] and therefore sought to improve on its efficiency in this current study. In this study, full-length human IgG1 mAb was constructed based on the amino acid sequence of the scFv previously constructed by our

research team. The non-coding GC-rich DNA fragment is a super "chromatin opening element" and plays an important role in mammalian gene expression [27, 28]. The two vectors, pMH3 and pCApuro, constructed on the GC-rich mechanism, were therefore employed to obtain stable transfected cells. The purpose why the four recombinant vectors were co-transfected into CHO-s cells at same ratio was to allow the four vectors to assemble randomly in CHO-s cells by electroporation method and eventually obtain stable transfectants with high yield by screening (Supplementary Fig. 2).

The Wave Bioreactor System used in this study was based on a novel oxygen (O_2) transfer method widely applied in large-scale fermentation of mammalian cells [29, 30]. To improve the expression and maintain the stability and activity of mAb-04, a relatively lower temperature of 34 °C was selected as the expression temperature (Supplementary Fig. 3). The impurity of purified mAb-04 was similar to that of Bevacizumab, a recombinant humanized anti-VEGF IgG1 antibody approved by FDA in 2004, which means the purified protein was approaching therapeutical grade for clinical application [31–33].

VEGFR2 binding assays and affinity determination demonstrated a potent binding capacity of mAb-04 to either the recombinant KDR3 or the KDR over-expressing cells HUVECs. We also used both in vitro and in vivo approaches to investigating the potential anti-angiogenic activities, according to the different stages of development of neo-vascularization. Firstly, it directly inhibited VEGF-stimulated HUVEC cells proliferation, migration, chemotactic motility and tube formation by cells on the Matrigel. Secondly, it suppressed new vessels growth in CAM. Considering the fact that homology of VEGFR2 from human and chicken is not high, and there is no formal proof to confirm mAb-04 can bind with VEGFR2 of chicken, the conclusion got from CAM is preliminary which needs further verification. The molecular mechanism of anti-angiogenic activity of mAb-04 in VEGF-induced angiogenesis was studied by Western blot, which demonstrated that mAb-04 blocked the VEGFR2 activation and suppressed the phosphorylation of ERK, AKT and P38 MAPK signaling pathway. This implies that mAb-04 can act as a promising anti-angiogenic full human IgG1 antibody. Since mAb-04 retained immune effector functions mediated by Fc domain, which was confirmed by the ADCC assay, we are interested in comparing the antineoplastic activities of mAb-04 and AK404R both in vitro and in vivo. In that respect, further studies are ongoing.

In conclusion, we have obtained a stable cell line which provided a novel full human mAb possessing unique amino acid sequence against the human VEGFR2 and magnified the fermentation in 5-L bioreactor. The robust design in vectors and vector combination produced a substantial improvement in yield and could potentially be applied to the development of multiple protein products. The full-length antibody candidate could be developed further as a novel antiangiogenic therapeutic antibody. The translation of anti-VEGFR2 antibody into clinical use will depend largely on successful in vivo preclinical tests and human clinical trials.

Acknowledgments This project was supported by the National Natural Science Foundation of China (NSFC81072561, NSFC81102364 and NSFC81273425). The Project Program of State Key Laboratory of Natural Medicines (China Pharmaceutical University, JKGP201101). Jiangsu Province Qinglan Project (2010). A Project Funded by the Priority Academic Program Development of Jiangsu Higher Education Institutions. Graduate Student Innovation Project Funded by Huahai Pharmaceutical Co. (CX13S-009HH). Revision by Professor Sherie L. Morrison.

Conflict of interest The authors declare that they have no conflict of interest.

References

1. Ozato K, Mayer N, Sachs DH (1980) Hybridoma cell lines screting monoclonal antibodies to mouse H-2 and la antigens. J Immunol 124(2):533–540
2. Yagami H, Kato H, Tsumoto K, Tomita M (2013) Monoclonal antibodies based on hybridoma technology. Pharm Pat Anal 2(2):249–263
3. Dubrot J, Portero A, Orive G, Hernández RM, Palazón A, Rouzaut A, Perez-Gracia JL, Hervás-Stubbs S, Pedraz JL, Melero I (2010) Delivery of immunostimulatory monoclonal antibodies by encapsulated hybridoma cells. Cancer Immunol Immunother 59(11):1621–1631
4. Tjandra JJ, Ramadi L, McKenzie IF (1990) Development of human anti-murine antibody (HAMA) response in patients. Immunol Cell Biol 68(6):367–376
5. Azinovic I, DeNardo GL, Lamborn KR, Mirick G, Goldstein D, Bradt BM, DeNardo SJ (2006) Survival benefit associated with human anti-mouse antibody (HAMA) in patients with B-cell malignancies. Cancer Immunol Immunother 55(12): 1451–1458
6. Morrison SL (1985) Transfectomas provide novel chimeric antibodies. Science 229(4719):1202–1207
7. Presta LG, Lahr SJ, Shields RL, Porter JP, Gorman CM, Fendly BM, Jardieu PM (1993) Humanization of an antibody directed against IgE. J Immunol 151(5):2623–2632
8. Winter G, Griffiths AD, Hawkins RE, Hoogenboom HR (1994) Making antibodies by phage display technology. Annu Rev Immunol 12:433–455
9. Cen X, Bi Q, Zhu S (2006) Construction of a large phage display antibody library by in vitro package and in vivo recombination. Appl Microbiol Biotechnol 71(5):767–772
10. Griffiths AD, Duncan AR (1998) Strategies for selection of selection of antibody phage display. Curr Opin Biotechnol 9(1):102–108
11. Dübel S, Stoevesandt O, Taussig MJ, Hust M (2010) Generating recombinant antibodies to the complete human proteome. Trends Biotechnol 28(7):333–339
12. Auguste P, Lemiere S, Larrieu-Lahargue F, Bikfalvi A (2005) Molecular mechanisms of tumor vascularization. Crit Rev Oncol Hematol 54(1):53–61

13. Kiselyov A, Balakin KV, Tkachenko SE (2007) VEGF/VEGFR signalling as a target for inhibiting angiogenesis. Expert Opin Investig Drugs 16(1):83–107
14. Roskoski R Jr (2007) Vascular endothelial growth factor (VEGF) signaling in tumor progression. Crit Rev in Oncol Hematol 62(3):179–213
15. Miao HQ, Hu K, Jimenez X, Navarro E, Zhang H, Lu D, Ludwig DL, Balderes P, Zhu Z (2006) Potent neutralization of VEGF biological activities with a fully human antibody Fab fragment directed against VEGF receptor 2. Biochem Biophys Res Commun 345(1):438–445
16. Zhang J, Li H, Wang X, Qi H, Miao X, Zhang T, Chen G, Wang M (2012) Phage-derived fully human antibody scFv fragment directed against human vascular endothelial growth factor receptor 2 blocked its interaction with VEGF. Biotechnol Prog 28(4):981–989
17. Carmeliet P (2003) Angiogenesis in health and disease. Nat Med 9(6):653–660
18. Folkman J, Shing Y (1992) Angiogenesis. J Biol Chem 267(16):10931–10934
19. Ziyad S, Iruela-Arispe ML (2011) Molecular mechanisms of tumor angiogenesis. Genes Cancer 2(12):1085–1096
20. Shibuya M, Claesson-Welsh L (2006) Signal transduction by VEGF receptors in regulation of angiogenesis and lymphangiogenesis. Exp Cell Res 312(5):549–560
21. Li H, Cao W, Chen Z, Acheampong DO, Jin H, Li D, Zhang J, Wang M (2013) The antiangiogenic activity of a soluble fragment of the VEGFR extracellular domain. Biomed Pharmacother 67(7):599–606
22. Wahl O, Oswald M, Tretzel L, Herres E, Arend J, Efferth T (2011) Inhibition of tumor angiogenesis by antibodies, synthetic small molecules and natural products. Curr Med Chem 18(21):3136–3155
23. Ferrara N, Kerbel RS (2005) Angiogenesis as a therapeutic target. Nature 438(7070):967–974
24. Saharinen P, Eklund L, Pulkki K, Bono P, Alitalo K (2011) VEGF and angiopoietin signaling in tumor angiogenesis and metastasis. Trends Mol Med 17(7):347–362
25. Ferrara N (2010) Pathways mediating VEGF-independent tumor angiogenesis. Cytokine Growth Factor Rev 21(1):21–26
26. Zhang J, Li H, Chen W, Cao P, Wang M (2009) Preparation of extracellular domain 3 of human VEGF receptor-2 and the monitoring of its real-time binding to VEGF by biosensors. Biotechnol Prog 25(6):1703–1708
27. Jia Q, Wu H, Zhou X et al (2010) A "GC-rich" method for mammalian gene expression: a dominant role of non-coding DNA GC content in regulation of mammalian gene expression. Sci China Life Sci 53(1):94–100
28. Zhang F, Zhou Z, Xu X, Wang X, Sullivan C (2008) A bizarre Jurassic maniraptoran from China with elongate ribbon-like feathers. Nature 455(7216):1105–1108
29. Kilani J, Lebeault JM (2007) Study of the oxygen transfer in a disposable flexible bioreactor with surface aeration in vibrated medium. Appl Microbiol Biotechnol 74(2):324–330
30. Warnock JN, Al-Rubeai M (2006) Bioreactor systems for the production of biopharmaceuticals from animal cells. Biotechnol Appl Biochem 45(1):1–12
31. Kaja S, Hilgenberg JD, Everett E, Olitsky SE, Gossage J, Koulen P (2011) Effects of dilution and prolonged storage with preservative in a polyethylene container on Bevacizumab (Avastin™) for topical delivery as a nasal spray in anti-hereditary hemorrhagic telangiectasia and related therapies. Hum Antibodies 20(3–4):95–101
32. Chen S 4th, Karnezis T, Davidson TM (2011) Safety of intranasal Bevacizumab (Avastin) treatment in patients with hereditary hemorrhagic telangiectasia-associated epistaxis. Laryngoscope 121(3):644–646
33. Karnezis TT, Davidson TM (2011) Efficacy of intranasal bevacizumab (Avastin) treatment in patients with hereditary hemorrhagic telangiectasia-associated epistaxis. Laryngoscope 121(3):636–638

View publication stats